

PAPER • OPEN ACCESS

Numerical and Experimental Study on Large Amplitude Sloshing Liquid Impact on Tank Roof

To cite this article: Haoran Qin *et al* 2019 *IOP Conf. Ser.: Earth Environ. Sci.* **242** 022066

View the [article online](#) for updates and enhancements.



IOP | ebooks™

Bringing you innovative digital publishing with leading voices to create your essential collection of books in STEM research.

Start exploring the collection - download the first chapter of every title for free.

Numerical and Experimental Study on Large Amplitude Sloshing Liquid Impact on Tank Roof

Haoran Qin¹, Yuan Hua^{1*} and Zhuang Wang^{1,2}

¹School of Environmental and Civil Engineering, Jiangnan University, Wuxi, Jiangsu, 214122, China

²State Key Laboratory of Hydrology-Water Resources and Hydraulic Engineering, Hohai University, Nanjing, Jiangsu, 210098, China

*Corresponding author's e-mail: huayuanxinxiang@126.com

Abstract. The smooth particle fluid dynamics (SPH) method and Finite Element (FEM) coupling algorithm are applied to study the problem of large sloshing impact cap in rectangular tank. The simulation results are compared with the experimental results. The results show that the numerical simulation results are in good consistent with the model test results. The feasibility and effectiveness of the method are verified. The liquid storage tank is more prone to liquid sloshing and impact capping under high liquid filling rate, and when the excitation frequency is approached to the first-order sloshing frequency of the liquid, the peak value of the sloshing increases as the amplitude of the sloshing increases, and the impact pressure process exhibits significant oscillation and random characteristics.

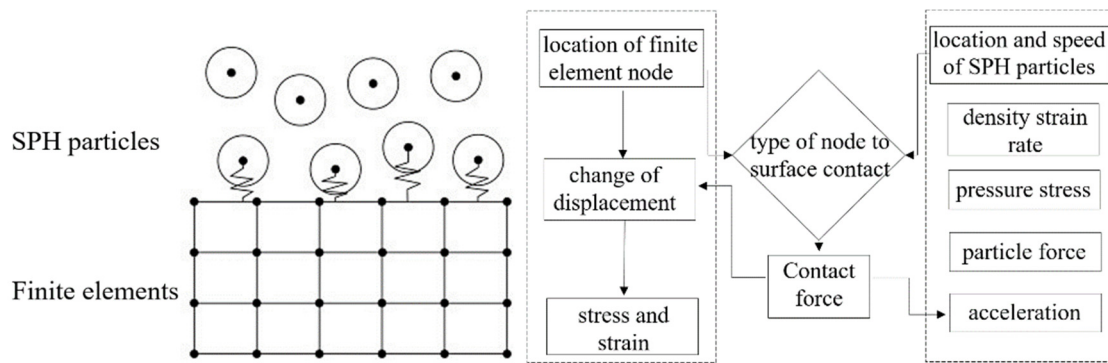
1. Introduction

The large sloshing impact of liquids involves a wide range of engineering fields, such as liquid cargo ship's tanks during voyages[1], oil tanks with floating roofs under earthquake impact[2] and tanks in reactor structures[3]. When the liquid in the various tank structures is greatly shaken, it not only exerts impact pressure on the side wall of the tank, but also can impact the tank roof[4]. At the same time, this impact capping phenomenon is generally more likely to occur in a liquid reservoir with a high liquid filling rate[5]. In the current study, the large sloshing liquid impact is more focused on the side wall impact study, while less attention is paid to the tank roof. In this paper, a combination of numerical and experimental methods is used. The numerical simulation uses the SPH-FEM coupling algorithm to simulate the large sloshing impact of the liquid in a rectangular tank. The simulation results are compared with the model test results, and the liquid impact tank roof was shaken sharply under different excitation parameters for further discussion.

2. SPH-FEM coupling algorithm

The SPH-FEM coupling algorithm is essentially a contact algorithm in which SPH particles are treated as special node units, and the control parameters are node number, quality, and spatial position. The coupling of SPH particles and FEM is to apply the force of the particle to the surface of the finite element by a penalty function. Therefore, the SPH-FEM coupling adopts the contact method of node-to-surface contact. In the SPH and FEM coupling process, the SPH particle is defined as the master node, and the finite element cell surface on the interface with the SPH particle is defined as the slave surface. The SPH-FEM coupling algorithm is shown in Figure 1.





(a) SPH particles and finite element contact

(b) SPH-FEM coupling algorithm flow

Figure 1. SPH-FEM coupling algorithm

In the numerical calculation, FEM uses the central difference scheme to solve the explicit dynamic equations, and the contact force is added to the SPH momentum equation and the finite element dynamic equation in the form of external force.

$$M\ddot{U} + CU + Kd = F + F_C \quad (1)$$

The contact force is calculated by reference to the meshless particle contact algorithm proposed by Vignjevic et al.[6]. The contact force applied to the joint between the node and the particle is calculated as follows:

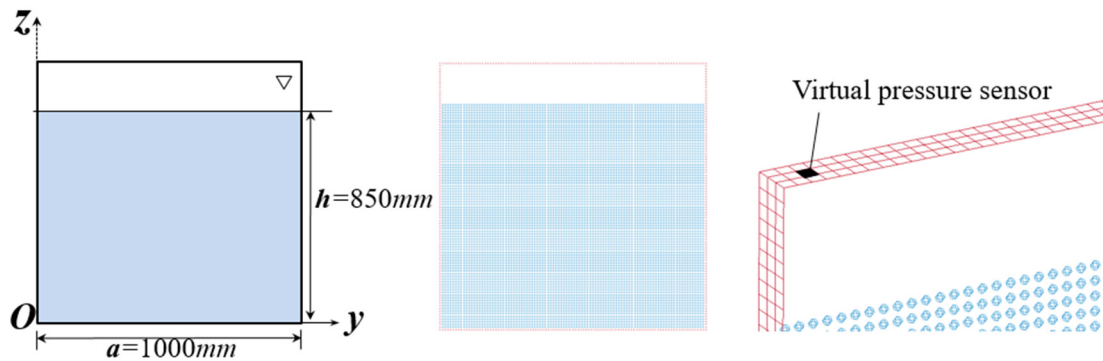
$$F_C = \sum_{j=1}^N \frac{m_j}{\rho_j} \cdot \frac{m_i}{\rho_i} KN \frac{W(r_i - r_j)^{N-1}}{W(h_{avg})^N} \cdot \nabla_j W(r_i - r_j) \quad (2)$$

In this formula, h_{avg} represents the average value of the smooth length between particles, K represents the contact stiffness.

3. Case analysis

3.1. Numerical model and calculation parameters

In this paper, the SPH-FEM coupling algorithm is used to simulate the movement of the liquid sloshing impact cap. The calculated geometry of the reservoir is shown in Figure 2(a). The tank width is 1000 mm, the height is 1000mm, and the liquid width in the tank is 30 mm, depth of the liquid is 850 mm. The initial numerical calculation model of the SPH-FEM coupling algorithm is shown in Figure 2(b). The fluid domain particles are arranged in a rectangular shape with an initial spacing of 10 mm. After the dispersion, a total of 8,500 SPH particles are obtained. Figure 2(c) shows the virtual pressure sensor arranged at the top of the tank, which is mainly used to obtain the impact force of the sloshing liquid on the tank roof.



(a) Tank geometry (b) SPH-FEM coupling calculation model (c) Virtual pressure sensor

Figure 2. Geometric shape and numerical calculation model of rectangular tank

Applying a transverse mode of harmonic excitation load at the wall of the tank: $Y=A\sin(2\pi ft)$, Excitation frequency $f=0.880$ Hz is the calculated first-order sloshing frequency of the fluid in the tank. The amplitudes of the excitation displacement are: $A=20$ mm, $A=30$ mm, $A=40$ mm, $A=50$ mm.

3.2. Tank test model and test conditions

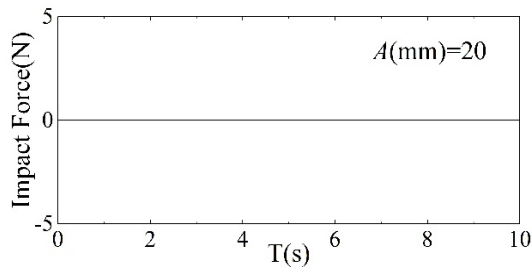


Figure 3. Rectangular tank model structure and shaking table

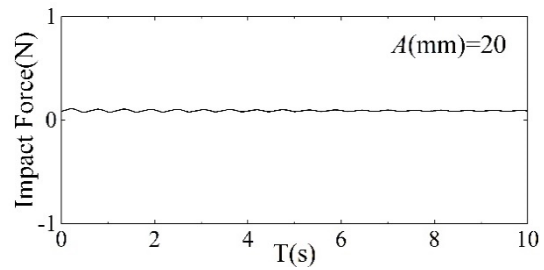
The testing device is mainly composed by a rectangular tank model, a horizontal single degree of freedom vibration table, data measurement and acquisition equipment, etc., as shown in Figure 3. The rectangular tank is fixedly placed on the horizontal vibration table. The liquid in the box is 1000 mm long and high, and the width is 30 mm, so as to avoid the three-dimensional effect of liquid sloshing and the viscous resistance of the side wall of the tank. At the same time, the tank structure is made with 10mm thick high-strength transparent plexiglass plate, and three stiffeners are installed around the tank to meet the requirements of rigid side wall to prevent the fluid-solid coupling between the tank wall and the fluid.

The filling depth of the rectangular tank is 850 mm, and the vibration table test adopts the simple harmonic excitation signal: $Y=A\sin(2\pi ft)$, loading in displacement mode. In the test condition, the sloshing frequency adopts $f=0.880$ Hz, and the amplitude of the excitation displacement is: $A=20$ mm, $A=30$ mm, $A=40$ mm, $A=50$ mm.

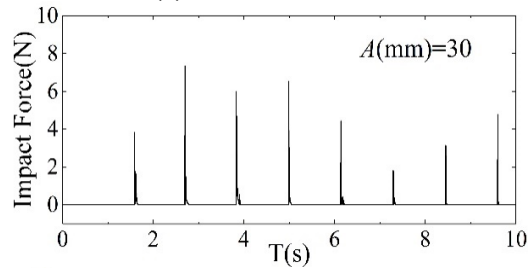
3.3. Calculation results and analysis



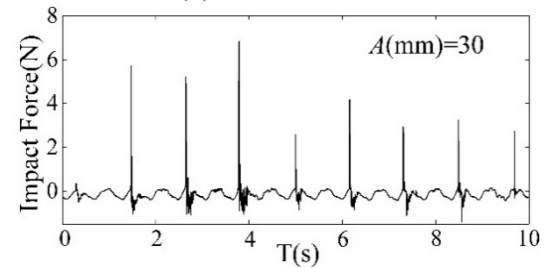
(a) Numerical results



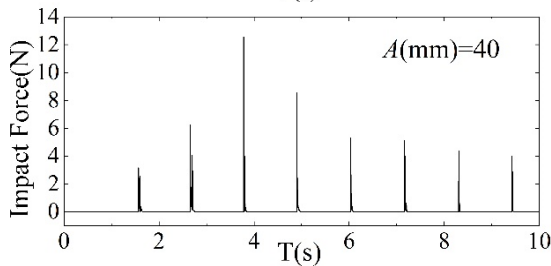
(b) Test results



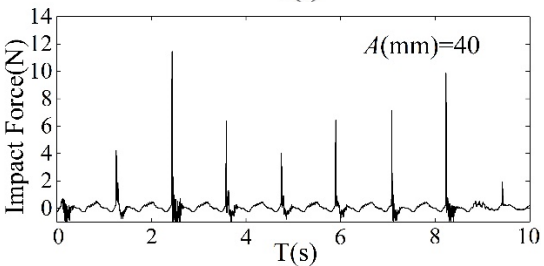
(a) Numerical results



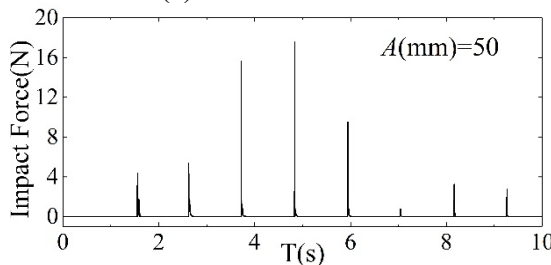
(b) Test results



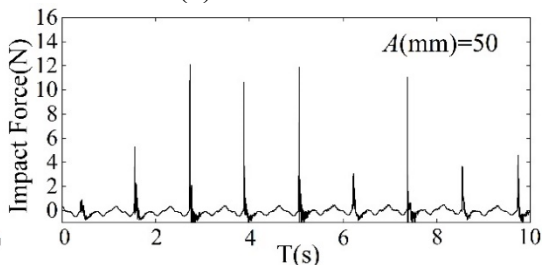
(a) Numerical results



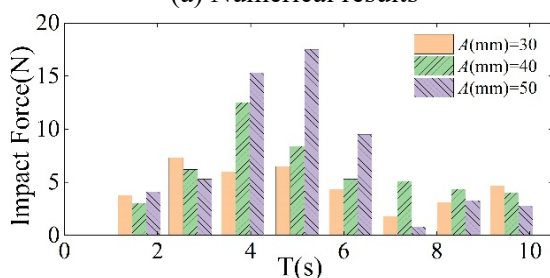
(b) Test results



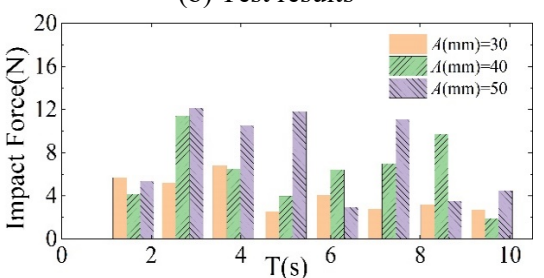
(a) Numerical results



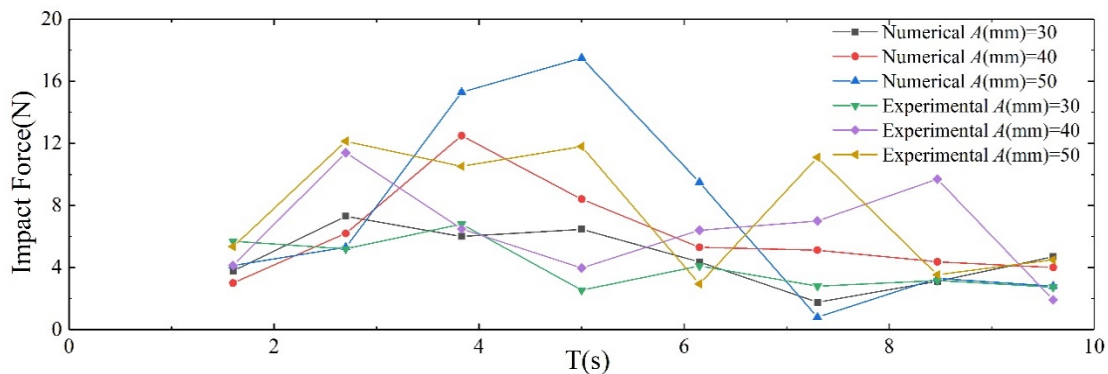
(b) Test results



(a) Numerical results



(b) Test results



(k) Numerical test results comparison

Figure 4. Large amplitude sloshing fluid roof impact pressure time history and peak contrast

Figure 4(a) to (j) show the impact time of the sloshing liquid of numerical calculations, experimental results and comparison charts under the condition of $f=0.880\text{Hz}$, displacement amplitude $A=20\text{ mm}$, $A=30\text{ mm}$, $A=40\text{ mm}$, $A=50\text{ mm}$. Figure 4(a), (c), (e), and (g) are time-history graphs of numerical calculation results, and Figure 4(i) is a barogram of pressure peaks corresponding to numerical results; Figure 4(b), (d), (f), (h) are the time-history curves of the test results, Figure 4 (j) is the corresponding pressure peak-contrast histogram of the test results; Figure 4 (k) is the curve diagram comparing the value of the peak impact pressure with the test results, it can be seen that when the amplitude value $A=50\text{ mm}$, the value of the impact pressure and the test result are too large, which is because the liquid sloshing impacts the tank roof at the same time when the magnitude of the excitation amplitude is large. The strong nonlinear phenomena such as breaking waves and flipping and the accompanying air pockets have certain limitations in the arrangement of the impact pressure sensor in the test, resulting in a large error in the test results of the impact pressure.

According to statistics, the peak value of the impact pressure in the numerical calculation results is 7.32N for the amplitude value $A=30\text{mm}$, 12.56N for the amplitude value $A=40\text{ mm}$, and 17.58N for the amplitude value $A=50\text{mm}$, which corresponds to the peak value of the impact pressure as a whole. The general rule that the value increases and increases. In the test results, the peak value of the impact pressure is 6.58N in the amplitude value $A=30\text{mm}$, 11.42N in the amplitude value $A=40\text{ mm}$, and 12.14 N in the amplitude value $A=50\text{ mm}$, which is smaller than the numerical result. In general, at the same excitation frequency, as the amplitude of the excitation displacement increases, the peak value of the impact pressure generated by the liquid on the tank roof increases accordingly, and the peak value of the impact pressure is oscillating and random.

4. Conclusion

In this paper, numerical simulation and experimental research on the impact of large amplitude liquid sloshing on the tank roof in a rectangular tank are carried out. The contact between the fluid and the tank roof is analyzed by the contact algorithm of meshless particles. The numerical simulation results are in agreement with the model test results. It is better to verify the rationality of the numerical model and the feasibility of the method. The following conclusions can be drawn from the example analysis:

(1) The SPH-FEM coupling algorithm can effectively describe the impact process on the tank top cover under the condition of large sloshing of the liquid, and solve the nonlinear sloshing problem with free liquid surface curl, crushing and large deformation, which is stable and efficient.

(2) Under the condition of high liquid filling rate, the liquid storage tank is more likely to slam the liquid to impact the tank roof, and when the excitation frequency is close to the first-order sloshing frequency range of the liquid in the tank, the amplitude of the shock increases and the peak value of impact pressure also increases significantly, and the impact pressure process exhibits oscillation and random characteristics.

Acknowledgment

This study was supported by the Natural Science Foundation of Jiangsu Province (BK20160184), the Fund of the State Key Laboratory of Hydrology-Water Resources and Hydraulic Engineering (2015491211) and the Fundamental Research Funds for the Central Universities (JUSRP11523).

References

- [1] Chen, G., Dong, S. (2016) Numerical simulation of liquid sloshing tank by CIP method. *Engineering mechanics*, 33(8): 1-7.
- [2] Sun, J.G., Cui, L.F., Hao, J.F., et al. (2013) The simplified mechanical model and the seismic response for isolation tank with floating roof. *Journal of Harbin Institute of technology*, 45(10): 118-122.
- [3] Zeng, X.J., Lu, D.G., Dang, J.J., et al. (2015) Research on sloshing characteristics in passive cooling storage tank of AP1000 under long-period earthquake. *Nuclear Power Engineering*, 36(5): 91-95.
- [4] Choi, H.L., Kwon, S.H., Park, J.H. et al. (2010) A study on the effect of filling ratio on sloshing impact pressure. *Journal of Ocean Engineering and Technology*, 24(6): 30-33.
- [5] Mehl, B., Püttmann, A., Sebastian, S. (2014) Sensitivity study on the influence of the filling height on the liquid sloshing behavior in a rectangular tank. In: *Proceedings of the Twenty-fourth International Ocean and Polar Engineering Conference*. Busan. 278-285.
- [6] Vignjevic, R., Vuyst, T.D., Campbell, J.C. (2007) A Frictionless Contact Algorithm for Meshless Methods. *Computer Modeling in Engineering and Sciences*, 13(1):107-112.